PCCP

Accepted Manuscript

ROYAL SOCIETY
OF CHEMISTRY

www.rsc.org/pccp

Insights into hydrogen bond donors promoted fixation of carbon dioxide with epoxides catalyzed by ionic liquids†

Mengshuai Liu,[a] Kunqi Gao,[a] Lin Liang,[c] Fangxiao Wang,[a] Lei Shi,[a] Li Sheng,*[a] and Jianmin Sun*[ba]

[a] *The Academy of Fundamental and Interdisciplinary Science, Harbin Institute of Technology, Harbin 150080, PR China*

[b] *State Key Laboratory of Urban Water Resource and Environment, Harbin Institute of Technology, Harbin 150080, PR China*

[c] *School of Life Science and Technology, Harbin Institute of Technology, Harbin 150080, PR China*

*Corresponding authors: Li Sheng, E-mail: shengli@hit.edu.cn; Jianmin Sun, E-mail: sunjm@hit.edu.cn;

Abstract: Catalytic coupling of carbon dioxide with epoxides to cyclic carbonates is an important reaction that has been receiving renewed interest. In this contribution, the cycloaddition reaction in the presence of various hydrogen bond donors (HBD) catalyzed by hydroxyl/carboxyl task-specific ionic liquids (ILs) were studied in detail. It was found that the activity of ILs could be significantly enhanced in the presence of ethylene glycol (EG), and EG/HEBimBr were the most efficient catalysts for the CO_2 cycloaddition to propylene oxide. Moreover, the binary catalysts were also efficiently versatile for the CO_2 cycloaddition to less active epoxides such as styrene oxide and cyclohexene oxide. Besides, the minimum energy paths for this hydrogen bond-promoted catalytic reaction were calculated using density functional theory (DFT) method. The DFT results suggested that the ring-closing reaction was the rate-determining step in the HEBimBr-catalyzed cycloaddition reaction but the EG addition could remarkably reduce its energy barrier as the formation of hydrogen bond between EG and oxygen atom of epoxides led this process along the standard S_N2 mechanism. As a result, the ring-opening reaction became the rate-determining step in the EG/HEBimBr-catalyzed cycloaddition reaction. The work reported herein helped the understanding and design of catalysts for efficient fixation of CO_2 to epoxides via hydrogen bond activation.

Keywords: Carbon dioxide; Ionic liquids; Hydrogen bond donors; Cyclic carbonates; DFT calculations.

1. Introduction

Carbon dioxide is the product of carbonaceous fuel combustion and human activities, ca.35 gigatonnes CO_2 were produced per year on a grand scale.[1] As a greenhouse gas, its increasing concentrations in the air are linked to global climate change. Hence, conversion of CO_2 into industrially useful chemicals has dual significances in view of both environmental protection and sustainable chemistry. One of the most promising strategies in this area is the synthesis of cyclic carbonates via the cycloaddition of epoxides and CO_2 (Scheme 1), especially the synthesis of propylene carbonate (PC) and ethylene carbonate (EC). The cycloaddition reaction is attractive in that the reaction is not only green for 100 % atom efficiency, but also cyclic carbonates are valuable fine chemicals which are widely used as solvents, starting materials and constituents of batteries.[2] Furthermore, ring opening polymerisation of cyclic carbonates also gives rise to polycarbonates, which are valuable structural and functional materials.[3]

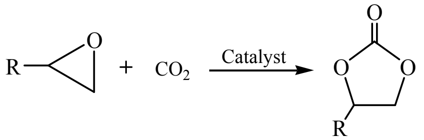

Scheme 1 Synthesis of cyclic carbonates from CO_2 and epoxides.

However, carbon dioxide is relatively stable and so unreactive having a standard heat of formation ($\Delta_f H_m^{\theta}$) of −393.5 kJ mol^{-1}.[4] Therefore, catalysts are needed to reduce the activation energy of any reaction in which it is involved. So far, quite numerous catalytic processes about the cycloaddition have been developed, ranging from homogeneous[5] to heterogeneous catalysts.[6] However, most of the catalysts usually suffer from low catalyst activity or additional solvent and high pressure/temperature, limiting their practicality. Thus, developing novel efficient catalysts for the cycloaddition reaction is highly desirable.

Recently, the unique characters of ILs such as thermal and chemical stability, selective solubility towards organic and inorganic materials, and high reusability of the catalysts, make ILs efficient solvent or catalysts for CO_2 cycloaddition to epoxides.[7] Peng firstly reported the quantitative conversion of propylene oxide (PO) to PC catalyzed by 1-butyl-3-methylimidazolium ($BMimBF_4$) ionic liquid.[8] Thereafter, imidazolium-,[9] ammonium-,[10] phosphonium-,[11] guanidinium-,[12] pyridinium-,[13] amino acid-,[14] Lewis base-,[15] polymeric[16] and immobilized ILs[17] were developed. Sun et al. demonstrated that when hydroxyl groups were added to the ILs, the cyclic carbonate yield were improved greatly.[18] Furthermore, hydroxyl-containing electrophile cooperated with metal salt catalysts were extensively explored[19] and theoretical studies demonstrated that the formation of hydrogen bonding between catalyst and epoxide could polarize and accelerate the ring-opening reaction of the epoxide.[20] However, due to the steric hindrance from cations of ILs, the activity needed to be further improved when taking economic efficiency into consideration. To the best of our knowledge, there is no report on systematic effect of hydrogen bond donors (HBD) cooperated with hydroxyl/carboxyl task-specific ionic liquids (ILs) on synthesis of cyclic carbonates. Herein, a series of task-specific ionic liquids with –OH/–COOH functional group were synthesized and characterized. The obtained ILs combined with various HBD were evaluated for the fixation of CO_2 to epoxides. The influences of ILs structures and reaction parameters on catalytic activity were investigated. A detailed mechanistic insight into conversion of propylene oxide with CO_2 was elucidated by DFT calculations, which provided us the detailed structural and energy information about each step of the catalytic process.

2. Experimental

2.1. General information

Carbon dioxide with purity of 99.99% was purchased from Harbin Qinghua Industrial gases Co. Ltd. PO, sodium hydride (60%), pyridine (99%), imidazole (99%), N-methylimidazole(99%), *n*-butyl bromide (≥99%), 2-bromoethanol (96%), bromoacetic acid (98%), tetrahydrofuran (extra dry, >99%) were purchased from Aladdin Chemical Co.. All other chemicals were purchased from Sinopharm Chemical Reagent Co., Ltd. with analytic grades and used without further purification.

^{1}HNMR spectra were detected on Bruker 400 spectrometer in D_2O (4.79 ppm) at ambient temperature. FT-IR spectra were measured on a PerkinElmer Spectrum 100 FT-IR Spectrometer. GC analyses were performed on Agilent GC-7890A equipped with a capillary column (Agilent 19091J-413) using flame ionization detector.

2.2. Synthesis of hydroxyl/carboxyl-containing ionic liquids

Six hydroxyl/carboxyl task-specific ionic liquids composed of Br^- anion (Scheme 2) were prepared according to the published procedures.[18, 21] And the detailed synthesis procedures and characterization results were described in ESI.†

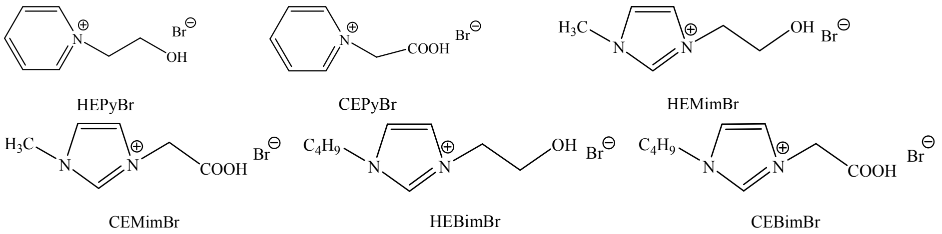

Scheme 2 Chemical structures of ILs used in this work and their designations.

2.3. General procedure for cyclic carbonate synthesis from epoxide and CO_2

In a typical run, the cycloaddition reaction was conducted in a 50 mL high pressure stainless-steel reactor that equipped with a magnetic stirring bar. Firstly, the reactor was purged with CO_2 to evacuate air, then a certain amount of IL, HBD and epoxide

(34.5 mmol) were added successively. Then, the reactor was heated, at the fixed reaction temperature, CO_2 was introduced into the reactor to a certain pressure, and the autoclave was heated at that temperature for a designated period of time. After the reaction was completed, the reactor was cooled to 0 °C in ice-water bath, and the remaining CO_2 was released. The product was extracted by ethyl acetate and analyzed on GC. And IL catalyst was separated by centrifugalization, washed with ethyl acetate (3 × 5 mL), and dried under vacuum. For the recycling experiments, additional fresh 10 mol% IL and recovered IL together with the fresh HBD were added for next run, because of the washing loss of IL.

2.4. Computational details

Within the framework of density functional theory (DFT), the equilibrium geometries of reactants, intermediates, transition states and products involved in the CO_2 cycloaddition were optimized using the recently developed M06-2X functionals combined with the standard 6-31G(d,p) basis set. The high accuracy of M06-2X for main-group thermochemistry and kinetics was already evaluated and recommended by Truhlar and co-workers.[22] The frequency calculations were also carried out at the M06-2X/6-31G(d,p) level of theory to confirm the nature of extreme point of the potential energy surface. That is, all the positive frequencies indicated stable structure and one imaginary frequency corresponded to the transition state. Finally, the minimum energy path (MEP) was constructed by intrinsic reaction coordinate (IRC) calculations. To evaluate the solvent effects and improve the reaction enthalpies and energy barriers, the energies were corrected by self-consistent reaction field (SCRF) method based on the polarized continuum model (PCM) at the M06-2X/6-311++G(2d,2p) levels of theory. In such PCM calculations, ethylene oxide parameters were used as the reaction takes place in PO rich phase but its accurate data lack at present. Zero-point energy (ZPE) was also taken into account in the energy corrections. The DFT calculations were performed using GAMESS program.[23]

3. Results and discussion

3.1. Activities of various catalysts for the cycloaddition reaction of CO_2 with PO

The activity of various –OH or –COOH containing ionic liquids as well as their synergetic effects with different HBD were investigated in the model reaction of CO_2 cycloaddition to PO, and the results were summarized in Table 1. The activities of single ILs on the reaction were moderate (entries 2–7). –OH containing ILs showed better catalytic activities than –COOH containing ILs, it was conjectured that –COOH showed stronger bound to Br^- than –OH group,[24] hence preventing from the nucleophilic attack of Br^-. For the same functional group and counterpart anion, the effect of the alkyl chain length in cation was not obvious (entry 4 *vs.* 6 and 5 *vs.* 7). and the best PC yield approached 67% with 99% selectivity under solvent free conditions of 140 °C and 2.0 MPa CO_2 for 2.5 h over HEBimBr catalyst (entry 6). Although theoretical studies reported that some cooperative effects between the –OH/or –COOH functional group and Lewis basic site of the IL played the important role in accelerating the synthesis of PC,[20,25] the steric hindrance existed in the cation structure and the electrostatic interaction between the ions[26] resulted in the reduced nucleophilicity of the anion, hindering the epoxide ring opening step. Thus, the catalytic activities over the bare ILs were still unsatisfactory. The effects of addition of HBD on the activities were investigated (entries 8–14). It was worth noting that HBD alone had no catalytic activity (entry 1) although it is an excellent activator to PO. The combination of HBD with HEBimBr realized the significant enhancement in activity compared with the separate HEBimBr (entries 11–14), indicating the necessary synergistic effects between HEBimBr and HBD on the acceleration of the activity. Especially with EG, the PC yield approached 94% with 99% selectivity under the same reaction conditions (entry 11 *vs.* entry 6). With the extension the reaction time, PC yield was improved to almost quantitative conversion of 98% (entry 15). The improvement was attributed to the integrated positive effects coming from imidazolium cation as well as EG acting as the acidic sites and bromine anion as the Lewis basic site, leading to the smooth ring-opening of epoxide by forming hydrogen bonds between the oxygen atom of PO and EG with IL (entries 11–14). Unfortunately, some HBD showed negligible effects on catalytic activities (entries 8–10), because they showed petty activation to PO and to some extent also limited the nucleophilicity of the anions.[24,26] In the case of ethyl alcohol, the strong intermolecular hydrogen bonds due to the strong polarization effect weakened its interaction to oxygen of PO (entry 8). Sucrose might be partly carbonized under reaction conditions, not resulting in the positive effect (entry 9). As to PEG-10000, the hydroxyl at the both ends of the chain could not effectively interact with oxygen of epoxide to promote the reaction. For the recyclability of ILs (entries 16-18), it was observed that the catalysts still exhibited high PC yield and selectivity in the 4th reuse, representing a reproducible catalyst for the cycloaddition of CO_2 and PO.

Table 1 Activities of various catalysts for the cycloaddition reaction of CO_2 with PO[a]

Entry	IL	HBD	Yield (%)[b]	Selectivity (%)[b]	TOF (h^{-1})[c]
1	–	EG	–	–	–
2	HEPyBr	–	63	99	58
3	CEPyBr	–	54	98	50
4	HEMimBr	–	65	99	60
5	CEMimBr	–	60	99	55
6	HEBimBr	–	67	99	62
7	CEBimBr	–	63	98	58
8	HEBimBr	Ethanol	64	97	59
9	HEBimBr	Sucrose	62	97	57
10	HEBimBr	PEG-10000	57	98	52
11	HEBimBr	EG	94	99	86
12	HEBimBr	H_2O	91	97	84
13	HEBimBr	Phenol	87	98	80
14	HEBimBr	Acetic acid	85	98	78

15[d]	HEBimBr	EG	98	99	75
16[e]	HEBimBr	EG	94	99	86
17[f]	HEBimBr	EG	93	99	86
18[g]	HEBimBr	EG	91	99	84

[a] Reaction conditions: PO (34.5 mmol), IL (0.15 mmol), HBD (0.60 mmol), 140 °C, 2.0 MPa, 2.5 h. [b] Based on GC analysis. [c] Moles of PC produced per mole of IL catalyst per hour. [d] t = 3.0 h. [e] 2nd –reuse. [f] 3rd –reuse. [g] 4th -reuse.

3.2. Effects of reaction parameters on PC synthesis

The influence of EG/HEBimBr molar ratio varied from 0 to 5:1 on PC yield was carried out in Table 2. With HEBimBr alone, 67% of PC yield was obtained (entry 1). While with the presence of EG, the activity of HEBimBr was sensitively improved. The PC yield remarkably increased with the molar ratio of EG/HEBimBr up to 4:1 and PC selectivities kept all about 99%, whereas further increase of EG resulted in a slight change in the product yield (entries 2–6). Thus, the optimum EG/HEBimBr molar ratio was 4:1. At the optimum molar ratio, the effect of reaction temperature on PC yield was investigated (entries 5, 7–10). There was no activity at 30 °C and when the temperature was increased to 80 °C, a very low yield of 17% was obtained with 99% selectivity. Excellent yield of 86% was achieved at 120 °C due to the increased homogeneity of the reaction system at elevated temperature, thereby furnishing more effective collisions of substrates with the catalysts. However, further increase the temperature to 160 °C caused a slight decrease in PC selectivity, presumably due to the side reaction such as isomerization of PO[24,27] as shown in Scheme 3. Therefore, the reaction temperature 140 °C was determined for further investigation.

Table 2 Effect of EG/HEBimBr molar ratio and reaction temperature on the PC yield[a]

Entry	Molar ratio	Temperature (°C)	Yield (%)[b]	Selectivity (%)[b]
1	–	140	67	99

2	1:1	140	69	99
3	2:1	140	76	99
4	3:1	140	89	99
5	4:1	140	94	99
6	5:1	140	95	99
7	4:1	30	trace	–
8	4:1	80	17	99
9	4:1	120	86	99
10	4:1	160	95	96

[a] Reaction conditions: PO (34.5 mmol), HEBimBr (0.15 mmol), 2.0 MPa, 2.5 h. [b] Based on GC analysis.

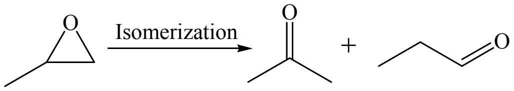

Scheme 3 Possible side reaction of PO.

Generally, a significant drawback of using CO_2 as reagent is the potential danger associated with high-pressure operations.[27] The effect of CO_2 pressure on the PC synthesis over EG/HEBimBr catalysts was exhibited in Fig. 1. The PC yield increased dramatically in the low-pressure range of 0.5–2.0 MPa at 140 °C, an increase in CO_2 pressure from 2.0 MPa to 3.0 MPa resulted in a slight increase in PC yield. According to the previous literatures,[28] the possible reason for the above phenomena was ascribed to the phase behavior of CO_2-PO system. There existed two phases including the bottom PO-rich liquid phase and the top CO_2-rich gas phase, and the reaction mainly took place in the liquid phase which dispersed the catalysts. With increasing CO_2 pressure, the concentration of CO_2 in the liquid phase enhanced thus leading to the increase of PC yield and PO conversion. However, the yield decreased as the pressure changed beyond 3.0 MPa up to 5.0 MPa, which was resulted from that too high pressure extracted more PO into the vapor phase and caused the reduced PO concentration in the vicinity of the catalysts, thus retarding the interaction between epoxide and the catalysts.[8,29] Conclusively, 2.0 MPa CO_2 was chosen for further investigation.

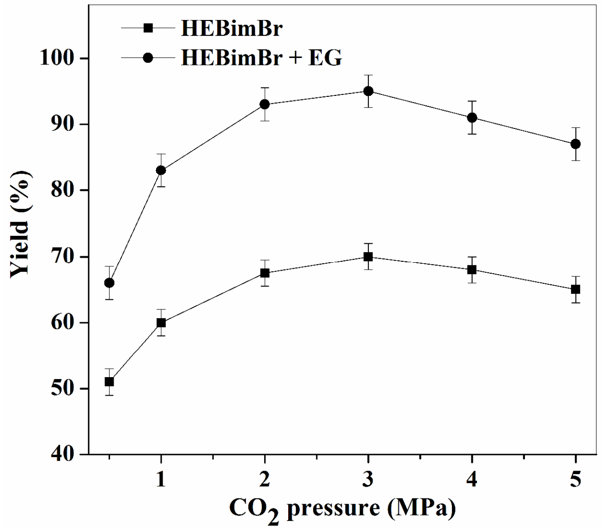

Fig. 1 The effect of CO_2 pressure on the PC synthesis. Conditions: PO (34.5 mmol), HEBimBr (0.15 mmol), EG (0.60 mmol), 140 °C, 2.5 h.

3.3. Computational studies on the reaction mechanism

In order to gain a deeper insight into the role of HBD, we performed the DFT calculations to investigate the HEBimBr- and EG/HEBimBr-catalyzed CO_2 cycloaddition process, respectively. Fig. 2 presented the calculated energy profiles over HEBimBr and EG/HEBimBr catalysts. The optimized structures for reactants, intermediates, transition states and products were displayed in Fig. 3 and Fig. 4, the cartesian coordinates of optimized geometries of stable points calculated at M06-2X/6-31G (d, p) level of theory were listed in ESI.† It can be seen that the hydrogen bond interaction between the catalysts and PO enhanced the reactivity of CO_2 cycloaddition. The energy barriers of ring-opening of PO were 21.2 ($TS_{A\text{-}B}$) and 21.1 ($TS_{F\text{-}G}$) kcal·mol^{-1} for HEBimBr- and EG/HEBimBr-catalyzed reactions, respectively, much lower than 59.0 kcal·mol^{-1} calculated for non-catalytic CO_2 cycloaddition.[25] That means, the EG addition barely affected the ring-opening process of PO. The next step was the coupling reaction of CO_2 and the activating PO. In Fig. 3, the structures of C, $TS_{C\text{-}D}$ and D showed an intermolecular hydrogen transfer process between O1 and C(2) atoms. The C(2)-H distances of C, $TS_{C\text{-}D}$ and D were 1.769, 1.228 and 1.086 Å. In the case of EG/HEBimBr, EG not only helped to activate the ring-opening reaction of epoxides but also stabilized the thereafter produced intermediates (see Fig. 4, structure G) with the stronger hydrogen bonds formed by the hydrogen atoms of EG and the activating oxygen atom of PO. As a result, the carbon atom of CO_2 easily bonded to the activated oxygen atom of PO, the energy barrier was only 1.9 ($TS_{H\text{-}I}$) $kcal\cdot mol^{-1}$. The last step was the formation of cyclic carbonate and the regeneration of catalysts, the energy barriers were respectively 41.1 $kcal\cdot mol^{-1}$ and 13.0 $kcal\cdot mol^{-1}$ for HEBimBr- and EG/HEBimBr-catalyzed processes. Obviously, the EG addition remarkably brought down the energy barrier and played a vital role in the ring-closing of epoxide. In Fig. 4, the $TS_{I\text{-}J}$ structure showed that O3 atom attacked the carbon atom at approximately 180^o to the leaving bromine atom. That is, the EG/HEBimBr-catalyzed reaction proceeded via the standard S_N2 mechanism, this way can minimize the steric hindrance of reaction. In contrast, the $TS_{D\text{-}E}$ structure (see Fig. 3) showed that in HEBimBr-catalyzed reaction, the attacking of O3 atom and leaving of the bromine atom took place on the same side. It means that this step possess a high energy barrier. Overall, the presented DFT calculations suggested that the ring-closing of PO was the rate-determining step with the largest energy barrier of 41.1 $kcal\cdot mol^{-1}$ over the HEBimBr catalyst. As compared with extra EG addition, the energy barrier of the ring-closing step dramatically decreased to 13.0 $kcal\cdot mol^{-1}$ and thus the ring-opening became the rate-determining step of EG/HEBimBr-catalyzed CO_2 cycloaddition reaction. This conclusion was also consistent with the theoretical study of CO_2 fixation with PO catalyzed by ammonium and guanidinium salts.[30]

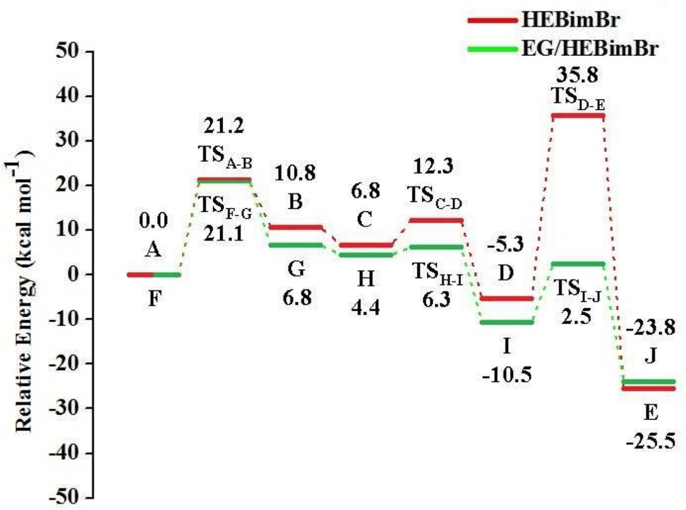

Fig. 2 Energy profile of minimum energy path (MEP) for HEBimBr- and EG/HEBimBr-catalyzed coupling reaction of PO with CO_2 calculated at the M06-2X/6-311++G(2d, 2p) level of theory. ZPE and the solvent effect were taken into account.

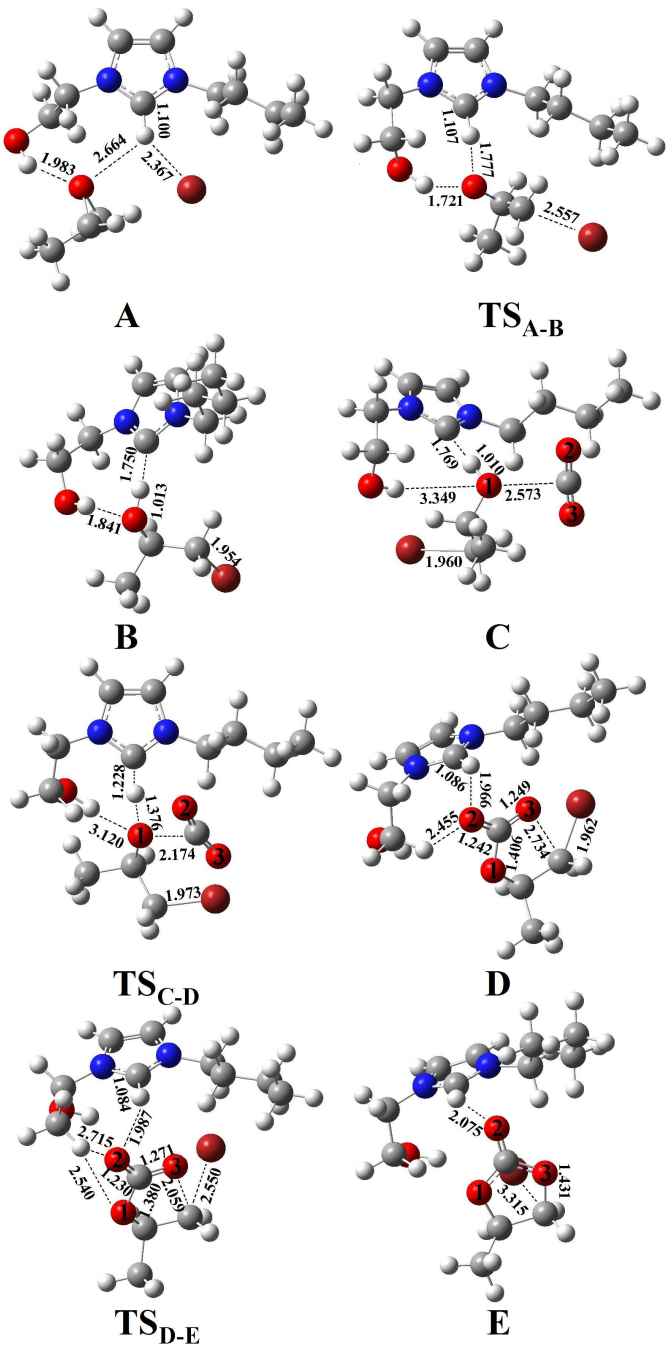

Fig. 3 The M06-2X/6-31G (d, p) optimized geometries of reactants, intermediates, transition states and products involving in the HEBimBr-catalyzed coupling reaction of PO with CO_2.

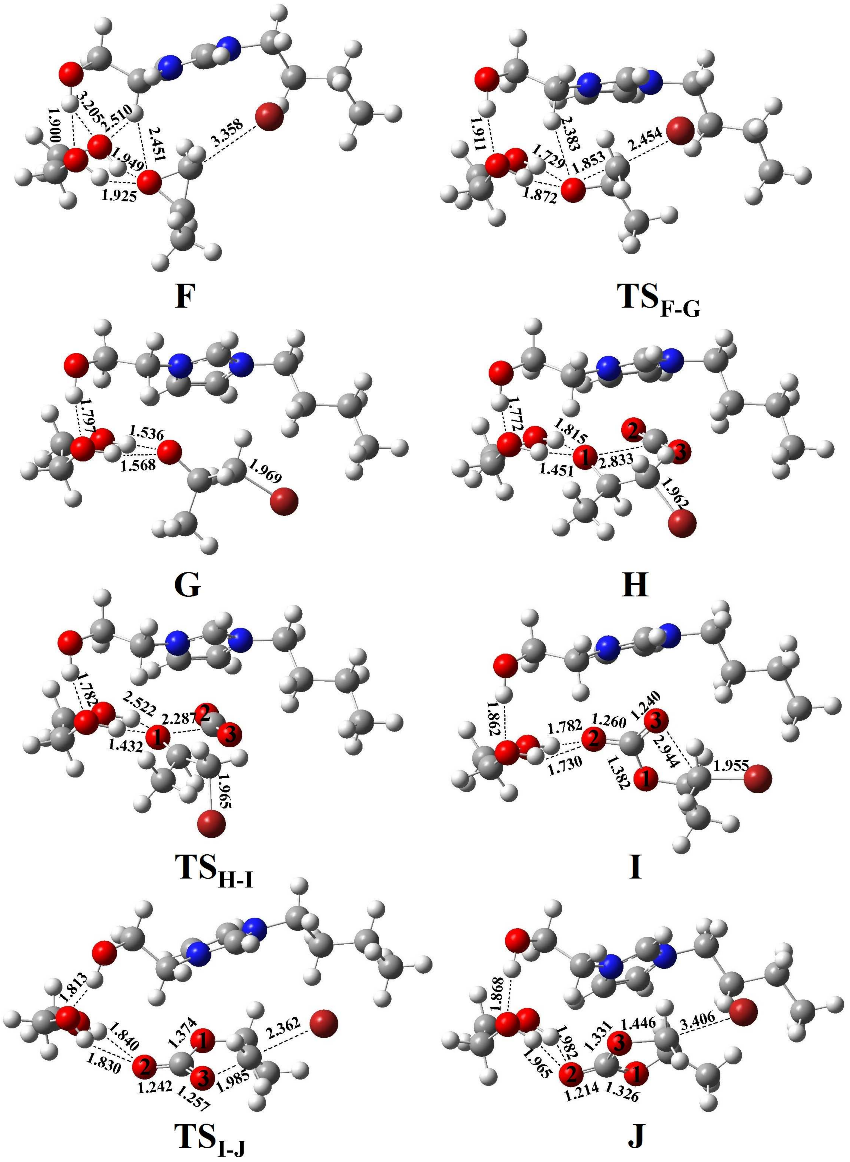

Fig. 4 The M06-2X/6-31G(d,p) optimized geometries of reactants, intermediates, transition states and products involving in the EG/HEBimBr-catalyzed coupling reaction of PO with CO_2.

Based on the DFT simulation results and previous literatures,[19] we proposed the plausible mechanism for the CO_2 cycloaddition to epoxides over EG/HEBimBr catalysts (Scheme 4). It was generally recognized that epoxide could be activated by forming hydrogen bonds with the oxygen of epoxide.[19,25] Thus, the hydroxy groups of EG and C(2)-H in IL cation firstly coordinated with the oxygen of epoxide through hydrogen bonds, resulting in the activation of epoxide molecule (Step 1). Simultaneously, the bromide anion as Lewis base nucleophilicly attacked on the less sterically hindered β-carbon atom of epoxide, facilitating the ring-opening of epoxide to obtain the intermediate oxyanion (I) (Step 2). Thereafter, CO_2 inserted (Step 3) into the intermediate (I) producing the new alkyl carbonate compound (II) (Step 4), which eventually afforded the cyclic carbonate and regenerated the catalysts by the subsequent intramolecular ring-closure (Step 5). Hence, the synergetic effects from EG of hydrogen bond donor, cation and anion of IL promoted the cycloaddition reaction smoothly.

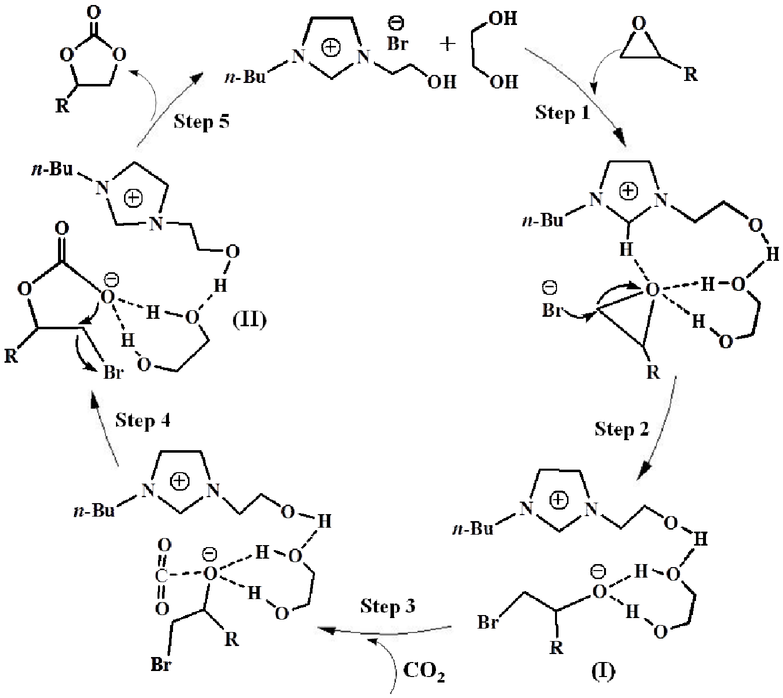

Scheme 4 Proposed mechanism for EG/HEBimBr catalyzed cycloaddition reaction of CO_2 and PO.

3.4. Catalytic activity towards CO_2 cycloaddition to other terminal epoxides

In order to show the potential and general applicability of EG/HEBimBr catalysts, the chemical fixation of CO_2 to different terminal epoxides was investigated and summarized in Table 3. EG/HEBimBr proved to be versatile for CO_2 cycloaddition to various epoxides giving the corresponding cyclic carbonates in good to excellent yields and selectivities. With the increase of the steric hindrance from epoxide, the catalytic activity was impeded. Especially for cyclohexene oxide, the crowded cyclohexene ring hindered the nucleophilic attack and thus caused the decreased activity of substrate (entry 4). Nonetheless, it was worth mentioning that the corresponding carbonate from cyclohexene oxide was obtained in excellent yield after longer reaction time of 6 h (entry 5). Thus the extension to various epoxides reflected the outstanding efficiency and generality of EG/HEBimBr catalysts.

Table 3 Coupling reaction of CO_2 with various epoxides catalyzed by EG/HEBimBr catalysts[a]

Entry	Epoxide	Product	T (°C)	t (h)	Reaction results[b]	
					Y_{PC} (%)	S_{PC} (%)
1	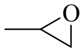	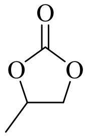	120	4.0	96	≥98
2	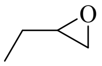	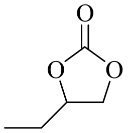	140	2.5	93	≥98
3	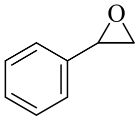	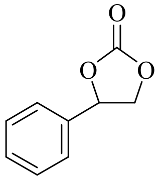	140	2.5	81	≥98
4	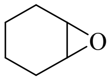	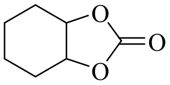	140	2.5	45	≥97
5	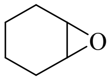	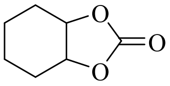	140	6.0	82	≥97

[a] Reaction conditions: epoxide (34.5 mmol), HEBimBr (0.15 mmol), EG (0.60 mmol), 2.0 MPa.

[b] Y_{PC}: PC yield; S_{PC}: PC selectivity; all based on GC analysis.

4. Conclusions

In summary, the systematic effects of different hydrogen bond donors cooperated with task-specific ionic liquids on synthesis of cyclic carbonates were thoroughly investigated. Experimental results and DFT studies suggested that the ring-closing reaction was the rate-determining step over HEBimBr catalyst. Additional HBD especially for EG, could remarkably decrease the energy barrier. As the hydrogen bond was formed between EG and oxygen atom of epoxides, which resulted in the ring-opening reaction became the rate-determining step in EG/HEBimBr-catalyzed cycloaddition reaction. EG played the vital roles in stabilizing intermediates and transition states through the strong hydrogen bond actions, thus promoting the cycloaddition reaction efficiently. Besides, the tentative mechanism in the presence of HBD catalyzed by hydroxyl/carboxyl containing ILs was proposed. The work reported herein would stimulate further research for efficient fixation of CO_2 to epoxides via hydrogen bond activation, and the mechanistic understanding for the process of CO_2 cycloaddition would provide insights into the rational design of robust catalytic systems for practical conversion of greenhouse gases into industrial chemicals.

Acknowledgements

We sincerely acknowledge the financial supports from National Natural Science Foundation of China (21373069), Science Foundation of Harbin City (NJ20140037), State Key Lab of Urban Water Resource and Environment of Harbin Institute of Technology (HIT2013TS01) and the Fundamental Research Funds for the Central Universities (HIT. IBRSEM. 201327).

References

1. D. J. Darensbourg and A. D. Yeung, *Polym. Chem.*, 2014, **5**, 3949–3962.
2. M. North, R. Pasquale and C. Young, *Green Chem.*, 2010, **12**, 1514–1539.
3. S. Supasitmongkol and P. Styring, *Catal. Sci. Technol*. 2014, **4**, 1622–1630.
4. C. E. Wartnaby, A. Stuck, Y. Y. Yeo and D. A. King, *J. Chem. Phys.*, 1995, **102**, 1855–1858.
5. (*a*) S. H. Kim, D. Ahn, M. J. Go, M. H. Park, M. Kim, J. Lee and Y. Kim, *Organometallics*, 2014, **33**, 2770–2775; (*b*) C. Beattie, M. North, P. Villuendas and C. Young, *J. Org. Chem.*, 2013, **78**, 419–426; (*c*) C. J. Whiteoak, N. Kielland, V. Laserna, F. C. Gómez, E. Martin, E. C.

Escudero-Adán, C. Bo and A. W. Kleij, *Chem. Eur. J.*, 2014, **20**, 2264–2275.

6. (*a*) W. Y. Gao, Y. Chen, Y. Niu, K. Williams, L. Cash, P. J. Perez, L. Wojtas, J. Cai, Y. S. Chen and S. Ma, *Angew. Chem. Int. Ed.*, 2014, **53**, 2615–2619; (*b*) Y. Xie, T. T. Wang, R. X. Yang, N. Y. Huang, K. Zou and W. Q. Deng, *ChemSusChem.*, 2014, **7**, 2110–2114; (*c*) R. A. Watile, K. M. Deshmukh, K. P. Dhake and B. M. Bhanage, *Catal. Sci. Technol.*, 2012, **2**, 1051–1055.
7. (*a*) S. Keskin, D. K. Talay, U. Akman and Ö. Hortaçsu, *J. Supercrit. Fluids*, 2007, **43**, 150–180; (*b*) H. O. Bourbigou, L. Magna and D. Morvan, *Appl. Catal. A: Gen.*, 2010, **373**, 1–56; (*c*) S. Chowdhury, R. S. Mohan and J. L. Scott, *Tetrahedron*, 2007, **63**, 2363–2389.
8. J. J. Peng and Y. Q. Deng, *New J. Chem.*, 2001, **25**, 639–641.
9. (*a*) J. N. Appaturi and F. Adam, *Appl. Catal. B: Environ.*, 2013, **136–137**, 150–159; (*b*) M. H. Anthofer, M. E. Wilhelm, M. Cokoja, I. I. E. Markovits, A. Pöthig, J. Mink, W. A. Herrmann and F. E. Kühn, *Catal. Sci. Technol.*, 2014, **4**, 1749–1758.
10. J. M. Sun, S. Fujita, B. M. Bhanage and M. Arai, *Catal. Today*, 2004, **93–95**, 383–388.
11. W. L. Dai, B. Jin, S. L. Luo, X. B. Luo, X. M. Tu and C. T. Au, *Appl. Catal. A: Gen.*, 2014, **470**, 183–188.
12. S. Foltran, J. Alsarraf, F. Robert, Y. Landais, E. Cloutet, H. Cramail and T. Tassaing, *Catal. Sci. Technol.*, 2013, **3**, 1046–1055.
13. W. L. Wong, P. H. Chan, Z. Y. Zhou, K. H. Lee, K. C. Cheung and K. Y. Wong, *ChemSusChem.*, 2008, **1**, 67–70.
14. Q. Gong, H. D. Luo, J. Gao, Y. H. Shang, H. B. Zhang, W. J. Wang and X. H. Zhou, *Aust. J. Chem.*, 2012, **65**, 381–386.
15. Z. Z. Yang, Y. N. Zhao, L. N. He, J. Gao and Z. S. Yin, *Green Chem.*, 2012, **14**, 519–527.
16. (*a*) S. Ghazali-Esfahani, H. Song, E. Păunescu, F. D. Bobbink, H. Liu, Z. Fei, G. Laurenczy, M. Bagherzadeh, N. Yan and P. J. Dyson, *Green Chem.*, 2013, **15**, 1584–1589; (*b*) T. Y. Shi, J. Q. Wang, J. Sun, M. H. Wang, W. G. Cheng and S. J. Zhang, *RSC Adv.*, 2013, **3**, 3726–3732; (*c*) Z. Z Yang, Y. F. Zhao, G. P. Ji, H. Y. Zhang, B. Yu, X. Gao and Z. M. Liu, *Green Chem.*, 2014, **16**, 3724–3728.
17. (*a*) D. W. Kim, K. A. Park, M. J. Kim, D. H. Kang, J. G. Yang and D. W. Park, *Appl. Catal. A: Gen.*, 2014, **473**, 31–40; (*b*) W. L. Dai, B. Jin, S. L. Luo, X. B. Luo, X. M. Tu and C. T. Au, *Catal. Sci. Technol.*, 2014, **4**, 556–562; (*c*) H. L. Shim, S. Udayakumar, J. I. Yu, I. Kim and D.

W. Park, *Catal. Today*, 2009, **148**, 350–354; (*d*) P. Agrigento, S. M. Al-Amsyar, B. Sorée, M. Taherimehr, M. Gruttadauria, C. Aprile and P. P. Pescarmona, *Catal. Sci. Technol.*, 2014, **4**, 1598–1607.

18. J. Sun, S. J. Zhang, W. G. Cheng and J. Y. Ren, *Tetrahedron Lett.*, 2008, **49**, 3588–3591.
19. (*a*) S. G. Liang, H. Z. Liu, T. Jiang, J. L. Song, G. Y. Yang and B. X. Han, *Chem. Commun.*, 2011, **47**, 2131–2133; (*b*) J. Sun, W. G. Cheng, Z. F. Yang, J. Q. Wang, T. T. Xu, J. Y. Xin and S. J. Zhang, *Green Chem.*, 2014, **16**, 3071–3078; (*c*) J. Tharun, G. Mathai, A. C. Kathalikkattil, R. Roshan, J. Y. Kwak and D. W. Park, *Green Chem.*, 2013, **15**, 1673–1677; (*d*) Z. Wu, H. Xie, X. Yu and E. Liu, *ChemCatChem.*, 2013, **5**, 1328–1333.
20. J. Q. Wang, J. Sun, W. G. Cheng, K. Dong, X. P. Zhang and S. J. Zhang, *Phys. Chem. Chem. Phys.*, 2012, **14**, 11021–11026.
21. L. F. Xiao, D. W. Lv and W. Wu, *Catal. Lett.*, 2011, **141**, 1838–1844.
22. (a) Y. Zhao and D. G. Truhlar, *Accounts Chem. Res.*, 2008, **41**, 157–167; (b) Y. Zhao and D. G. Truhlar, *Chem. Phys. Lett.*, 2011, **502**, 1–13.
23. M. W. Schmidt, K. K. Baldridge, J. A. Boatz, S. T. Elbert, M. S. Gordon, J. H. Jensen, S. Koseki, N. Matsunaga, K. A. Nguyen, S. J. Su, T. L. Windus, M. Dupuis, and J. A. Montgomery, *J. Comput. Chem*. 1993, **14**, 1347–1363.
24. J. Sun, L. J. Han, W. G. Cheng, J. Q. Wang, X P. Zhang and S. J. Zhang, *ChemSusChem*, 2011, **4**, 502–507.
25. L. Wang, X. F. Jin, P. Li, J. L. Zhang, H. Y. He and S. J. Zhang, *Ind. Eng. Chem. Res.*, 2014, **53**, 8426–8435.
26. N. N. Lichtin and K. N. Rao, *J. Am. Chem. Soc.*, 1961, **83**, 2417–2424.
27. C. X. Miao, J. Q. Wang, Y. Wu, Y. Du and L. N. He, *ChemSusChem.*, 2008, **1**, 236–241.
28. (*a*) Y. Y. Zhang, S. F. Yin, S. L. Luo, C. T. Au, *Ind. Eng. Chem. Res*., 2012, **51**, 3951–3957; (*b*) Y. Xie, Z. F. Zhang, T. Jiang, J. L. He, B. X. Han, T. B. Wu and K. L. Ding, *Angew. Chem. Int. Ed.*, 2007, **46**, 7255–7258.
29. H. Kawanami, A. Sasaki, K. Matsui and Y. Ikushima, *Chem. Commun.*, 2003, 896–897.
30. S. Foltran, R. Mereau and T. Tassaing, *Catal. Sci. Technol.*, 2014, **4**, 1585–1597.